

# Semantic Anchoring for Robust Personalization in Text-to-Image Diffusion Models

Seoyun Yang\* Gihoon Kim\* Taesup Kim†

Graduate School of Data Science, Seoul National University

## Abstract

*Text-to-image diffusion models have achieved remarkable progress in generating diverse and realistic images from textual descriptions. However, they still struggle with personalization, which requires adapting a pretrained model to depict user-specific subjects from only a few reference images. The key challenge lies in learning a new visual concept from a limited number of reference images while preserving the pretrained semantic prior that maintains text-image alignment. When the model focuses on subject fidelity, it tends to overfit the limited reference images and fails to leverage the pretrained distribution. Conversely, emphasizing prior preservation maintains semantic consistency but prevents the model from learning new personalized attributes. Building on these observations, we propose the personalization process through a semantic anchoring that guides adaptation by grounding new concepts in their corresponding distributions. We therefore reformulate personalization as the process of learning a rare concept guided by its frequent counterpart through semantic anchoring. This anchoring encourages the model to adapt new concepts in a stable and controlled manner, expanding the pretrained distribution toward personalized regions while preserving its semantic structure. As a result, the proposed method achieves stable adaptation and consistent improvements in both subject fidelity and text–image alignment compared to baseline methods. Extensive experiments and ablation studies further demonstrate the robustness and effectiveness of the proposed anchoring strategy.*

## 1. Introduction

Personalized content generation is a major application in image generative models [5, 30]. Rather than relying on samples drawn from the learned distribution, personalization aims to introduce subject-specific attributes into the generation process. Recent advancements in text-to-

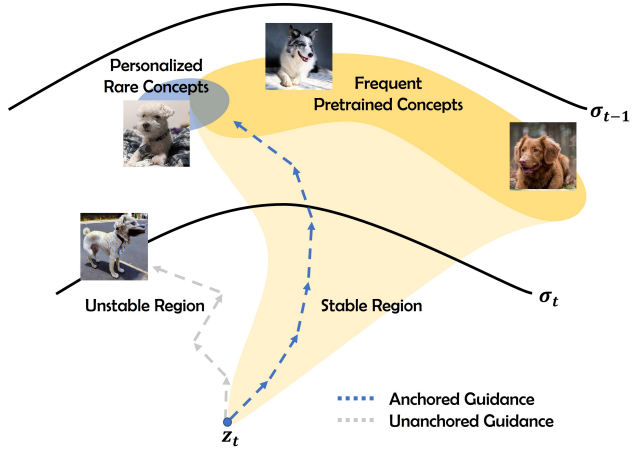


Figure 1. Conceptual illustration of the proposed method. pretrained semantics provide stable guidance, whereas guidance in newly introduced regions remains unstable. Our approach anchors personalization to the pretrained semantics, enabling stable guidance as the model expands toward novel concepts.

image diffusion models [4, 22, 27–29, 33] have highlighted strong foundation models for personalized content generation. Building on the success of text-to-image synthesis, personalization methods incorporate additional semantics to ensure that target attributes are reflected across diverse contexts of the pretrained distribution.

However, the limited number of reference images available for personalization presents a significant challenge. Instead of integrating novel features into the learned distribution, the model often overfits to the reference images and loses the knowledge encoded in the original distribution. To mitigate this issue, existing methods constrain the outputs of the pretrained model to prevent such drift. These approaches include selective layer updates [12, 38], additional normalization [6, 25], and parameter-efficient modules [9]. While restricting parameter updates enhances training stability, it also limits sufficient learning of target attributes.

Consequently, recent studies in personalization go beyond learning the denoising process for novel concepts and instead focus on guidance mechanisms that steer genera-

\*Equal contribution.

†Corresponding author.

tion toward the intended semantics during inference [20, 21], guiding the personalized guidance with the unconditional guidance of the original pretrained model based on Classifier-Free Guidance [2, 7, 11, 13]. The core question has thus shifted from how well the model reconstructs the concept to how effectively it can guide generation toward the personalized semantics.

Extending this perspective, we find that rare concept generation [31, 32, 39] addresses a similar underlying problem, where the goal is to enable stable generation of underrepresented concepts in the training distribution. In particular, Rare-to-Frequent [19] shows that inference-time guidance from frequent concepts enables stable generation of rare ones, indicating that capturing fine-grained details alone is insufficient and that effective generation requires expanding from general concepts toward specific representations. This insight suggests that personalization, which involves learning novel concepts beyond the pretrained distribution, shares the same underlying principle.

Nevertheless, existing personalization methods overlook the importance of maintaining the relationship between general and subject-specific concepts. While Beyond Fine-tuning [35] apply general guidance to personalization, their approach operates only at inference time, leaving the model unable to preserve semantic consistency throughout training. As a result, the alignment between personalized and pretrained semantics remains an open problem toward learning reliable personalized guidance.

In this paper, we introduce a training-time personalization objective that explicitly models the interaction between general and subject-specific representations. We first observe that the relationship between general and specific concepts progressively collapses as personalization proceeds, indicating that the personalized guidance suffers from semantic drift and loses alignment with the pretrained distribution. Therefore, we propose Semantic Anchoring Personalization, a relationship-aware objective that moves beyond learning isolated attributes and explicitly models the interaction between general and specific representations. Our approach refines the optimal solution of personalization objectives extending from the pretrained semantic structure toward fine-grained subject learning as illustrated in Figure 1. Quantitative and qualitative results demonstrate the robustness and general applicability of the proposed method, while ablation studies further validate its superior balance between subject fidelity and contextual generalization. In summary, our main contributions are as follows:

- We conceptualize diffusion-based personalization as a problem of learning rare concept generation that expands upon a pretrained semantic foundation.
- We propose Semantic Anchoring Personalization, which reformulates the objective beyond simple reconstruction to preserve the relationship between general and subject-

specific semantics through a semantic anchor.

- Our experiments and analyses demonstrate that our method achieves consistent improvements in fidelity and generalization across diverse backbones and outperforms existing baselines.

## 2. Related Work

### 2.1. Personalized Text-to-Image Generation

DreamBooth [30] is an early personalization method that trains all model parameters. Although it produces high-fidelity results, it often suffers from overfitting to the limited reference images. Textual Inversion [5], on the other hand, optimizes only a token-level representation, which leads to limited expressiveness. These limitations motivate subsequent research to explore strategies for selective parameter fine-tuning during personalization. Custom Diffusion [12] trains only the attention heads, while LoRA [9] adopts a low-rank adaptation strategy. Other studies modify specific components such as singular values [6] or angular features [25] of weight matrices to achieve lightweight yet effective adaptation. Although these approaches prevent a significant shift from the pretrained distribution and ensure stable optimization, they often limit the expressiveness toward target attributes.

Further approaches aim to enhance personalization by introducing new conditioners [34] or leveraging external networks [23, 41]. IP-Adapter [40] introduces a new conditioner trained from scratch to inject novel visual feature into the pretrained model. BLIP-Diffusion [14] utilizes vision-language models [15, 16] to guide the personalization process. These encoder-based methods improve conditioning flexibility through auxiliary encoders but require extensive computational resources and limits their per-subject adaptability. Moreover, their reliance on specific backbone architectures makes it difficult to generalize the approach across different diffusion models. These limitations highlight the need for a more principled training framework for diffusion-based personalization.

### 2.2. Semantic Guidance in Personalization

Recent personalization studies have shifted their focus from learning the denoising process to designing guidance mechanisms that steer generation toward the intended semantics. For instance, Park et al. [20] and Phunyaphibarn et al. [21] leverage pretrained unconditional guidance as an inference-time control signal. However, the effectiveness of such guidance depends on the conditional branch preserving the intended semantics. Once the conditional guidance drifts, the unconditional signal can no longer provide meaningful control. Achieving precise and semantically coherent guidance poses the same underlying challenge as rare concept generation [31, 32, 39]. Notably, Rare-to-Frequent

(R2F) [19] leverages guidance from frequent concepts to stabilize the synthesis of rare concepts. R2F establishes a sampling strategy that interpolates between well-learned and underrepresented concepts, reducing generative uncertainty and enabling more reliable synthesis of rare concepts.

Although previous personalization methods incorporate general information, they do so only to preserve pretrained semantics [30, 38] or to cover superclass-level representations [10, 24]. However, these approaches overlook the interactive relationship between pretrained and personalized representations, which hinders the integration of general semantics with novel concepts. Beyond-Finetuning [35] is the only work that interprets the subject as a rare concept and its superclass as a frequent one to guide personalization. However, since the guidance is applied only in inference time, it fails to maintain the semantic relationship between general and specific concepts. To address this gap, we introduce a training-time objective that ensures consistent alignment between general and subject-specific representations during personalization.

### 3. Method

In this section, we first introduce the notation and the baseline formulation used in personalization. Next, in Section 3.2, we empirically show that the personalized guidance fails to preserve the relationship between existing guidance. Finally, we reformulate the objective to build upon this relationship through semantic anchoring.

#### 3.1. Preliminary

**Text-to-Image Diffusion.** Text-to-image (T2I) diffusion models learn to generate an image latent  $z_0$  from a textual condition  $c$  by reversing a gradual noising process [8, 17, 18, 36, 37]. At each diffusion timestep  $t$ , a noisy latent  $z_t$  is obtained as  $z_t = \alpha_t z_t + \sigma_t \epsilon$ ,  $\epsilon \sim \mathcal{N}(0, I)$ , where  $\alpha_t$  and  $\sigma_t$  control the signal-to-noise ratio, and  $\epsilon$  denotes the ground-truth noise. A denoising network  $\epsilon_\theta(z_t, c, t)$  is trained to predict  $\epsilon$  so that the model can reconstruct the clean latent through iterative denoising steps. This training is also formulated as a noise-prediction objective [8]:

$$\mathcal{L}_{\text{diffusion}} = \mathbb{E}_{z_t, c, \epsilon, t} [\|\epsilon - \epsilon_\theta(z_t, c, t)\|_2^2].$$

**Personalization Setup.** Personalization adapts a pretrained T2I diffusion model parameterized by  $\theta'$  into a new model  $\theta$  capable of synthesizing images of a specific subject given only a few reference samples. Let  $c^{\text{sbj}}$  denote the subject prompt (e.g., “a photo of a [V\*] dog”), where [V\*] denotes a special token representing the subject attribute. The personalized model is trained with the same reconstruction-based objective, which enforces accurate denoising for the target subject:

$$\mathcal{L}_{\text{recon}} = \mathbb{E}_{z_t, c^{\text{sbj}}, \epsilon, t} [\|\epsilon - \epsilon_\theta(z_t, c^{\text{sbj}}, t)\|_2^2]. \quad (1)$$

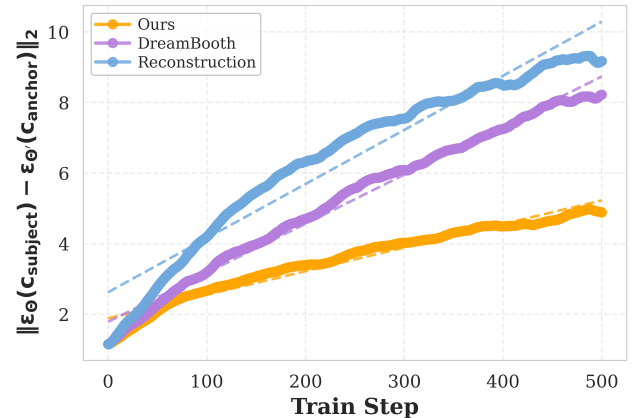


Figure 2.  $L_2$  distance between subject prediction  $\epsilon_\theta(z_t, c^{\text{sbj}}, t)$  and  $\epsilon_{\theta'}(z_t^{\text{cls}}, c^{\text{cls}}, t)$  anchor prediction measured over adaptation steps.

Training with this objective makes it difficult for the personalized model to preserve the original distribution. To alleviate this issue, DreamBooth [30] introduces a *Prior Preservation Loss* (PPL), which regularizes the model to maintain its pretrained knowledge. In practice, a superclass prompt  $c^{\text{cls}}$  (e.g., “a photo of a dog”) is used to generate class-level samples  $z_t^{\text{cls}}$  from the pretrained model  $\theta'$ , which are also reconstructed during personalization:

$$\mathcal{L}_{\text{ppl}} = \mathbb{E}_{z_t^{\text{cls}} \sim p_{\theta'}(c^{\text{cls}}, c^{\text{cls}}, \epsilon, t)} [\|\epsilon - \epsilon_\theta(z_t^{\text{cls}}, c^{\text{cls}}, t)\|_2^2]. \quad (2)$$

#### 3.2. Motivation

While the combination of Eq. (1) and Eq. (2) has become the standard training scheme for diffusion-based personalization, it does not consider the interaction between subject-specific (i.e., rare concept) and class-level (i.e., frequent concept) semantics. Each objective independently reconstructs  $z_t$  and  $z_t^{\text{cls}}$  with respect to  $c^{\text{sbj}}$  and  $c^{\text{cls}}$  without accounting for their mutual relationship.

To identify whether this alignment is preserved during personalization, we analyze the behavior of  $c^{\text{sbj}}$  and its prior  $c^{\text{cls}}$ . As shown in Figure 2, the subject-specific semantics gradually diverge from the frequent semantics  $\epsilon_{\theta'}(z_t^{\text{cls}}, c^{\text{cls}}, t)$ , and Eq. (2) fails to effectively mitigate this drift. This observation suggests that the existing personalization process fails to retain semantic drift between the personalized and pretrained representations. Such divergence represents a decoupling of the relationship between general and subject-specific semantics, which may lead to increased instability in subject-specific guidance as illustrated in Figure 1.

#### 3.3. Semantic Anchoring Personalization

To address the issue identified in Section 3.2, we reformulate the Rare-to-Frequent (R2F) [19] principle in the context of personalization. R2F demonstrates that interpolating

the score field of a rare concept with that of a frequent one provides more stable guidance for rare concept generation. Specifically, the conditional score for the blended concept is defined as

$$\lambda \nabla_x \log p(x|c^{\text{rar}}) + (1 - \lambda) \nabla_x \log p(x|c^{\text{frq}}),$$

where  $c^{\text{rar}}$  and  $c^{\text{frq}}$  denote the rare and frequent concepts, respectively. Here,  $\lambda \in [0, 1]$  is an interpolation coefficient that controls the relative contribution of the two conditional scores. Using Tweedie's formula [3, 37], which connects the posterior mean to the score function, the corresponding blended noise target for this equation can be expressed as

$$\epsilon^* = \lambda \epsilon^{\text{rar}} + (1 - \lambda) \epsilon^{\text{frq}}. \quad (3)$$

This formulation implies that the transition noise target for rare concept generation should not rely solely on reconstructing the reference samples but must also incorporate semantic guidance drawn from the frequent prior.

However, this principle has previously been applied only as an inference-time guidance mechanism. Directly applying this inference-time scheme to the personalization problem, however, presents a fundamental limitation. It fails to address the underlying issue identified in Section 3.2: the semantic drift that occurs during the adaptation process itself.

Thus, we reformulate this inference-time guidance principle as a training-time objective. Our goal is to train the personalized model to directly predict the ideal blended target  $\epsilon^*$  at training time. We achieve this by substituting the blended noise target  $\epsilon^*$  from Eq. (3) for the original noise  $\epsilon$  in the standard diffusion objective in Eq. (1), which yields the blended objective:

$$\mathbb{E} \left[ \left\| \underbrace{\lambda \epsilon^{\text{rar}} + (1 - \lambda) \epsilon^{\text{frq}} - \epsilon_\theta(z_t, c^{\text{sbj}}, t)} \right\|_2^2 \right].$$

Expanding the squared term yields

$$\epsilon_\theta - (\lambda \epsilon^{\text{rar}} + (1 - \lambda) \epsilon^{\text{frq}}) = \lambda(\epsilon_\theta - \epsilon^{\text{rar}}) + (1 - \lambda)(\epsilon_\theta - \epsilon^{\text{frq}}).$$

For clarity, let  $A = \epsilon_\theta - \epsilon^{\text{rar}}$ ,  $B = \epsilon_\theta - \epsilon^{\text{frq}}$ . Then,

$$\begin{aligned} \|\lambda A + (1 - \lambda) B\|_2^2 &= \lambda^2 \|A\|_2^2 + (1 - \lambda)^2 \|B\|_2^2 \\ &\quad + 2\lambda(1 - \lambda) \langle A, B \rangle. \end{aligned}$$

Using  $\langle A, B \rangle = \frac{1}{2}(\|A\|^2 + \|B\|^2 - \|A - B\|^2)$ , we obtain

$$\lambda \|A\|_2^2 + (1 - \lambda) \|B\|_2^2 - \lambda(1 - \lambda) \|A - B\|_2^2. \quad (4)$$

Substituting back into Eq. (4) yields

$$\lambda \|\epsilon_\theta - \epsilon^{\text{rar}}\|_2^2 + (1 - \lambda) \|\epsilon_\theta - \epsilon^{\text{frq}}\|_2^2 - \lambda(1 - \lambda) \|\epsilon^{\text{rar}} - \epsilon^{\text{frq}}\|_2^2.$$

Since the last term  $\lambda(1 - \lambda) \|\epsilon^{\text{rar}} - \epsilon^{\text{frq}}\|_2^2$  is independent of the trainable parameters  $\theta$ , it can be dropped during optimization. Normalizing by  $\lambda > 0$  yields the objective:

$$\mathcal{L} = \mathbb{E} \|\epsilon^{\text{rar}} - \epsilon_\theta\|_2^2 + \frac{1 - \lambda}{\lambda} \mathbb{E} \|\epsilon_\theta - \epsilon^{\text{frq}}\|_2^2.$$

This indicates a learnable rare-concept objective anchored by the pretrained frequent concept. We extend this formulation to personalization, where the model learns to adapt from the pretrained distribution toward subject-specific attribute while remaining anchored to the general semantics.

Here,  $\epsilon^{\text{rar}}$  denotes the ground-truth noise obtained from the reference (rare) images, and  $\epsilon^{\text{frq}}$  represents the pretrained prediction corresponding to the anchoring (frequent) concept  $c^{\text{anc}}$ . In this context,  $\epsilon^{\text{rar}}$  corresponds to the reconstruction target  $\epsilon$  used for the subject in Eq. (1).  $\epsilon^{\text{frq}}$  corresponds to the pretrained general semantic anchor  $\epsilon_{\theta'}(z_t, c^{\text{anc}}, t)$ , where  $c^{\text{anc}}$  is instantiated as the superclass prompt  $c^{\text{cls}}$ . The final training objective is defined as:

$$\begin{aligned} \mathcal{L} = \mathbb{E}_{z, c^{\text{sbj}}, c^{\text{anc}}, \epsilon, t} & \left[ \left\| \epsilon - \epsilon_\theta(z_t, c^{\text{sbj}}, t) \right\|_2^2 \right. \\ & \left. + w \left\| \epsilon_\theta(z_t, c^{\text{sbj}}, t) - \epsilon_{\theta'}(z_t, c^{\text{cls}}, t) \right\|_2^2 \right], \end{aligned} \quad (5)$$

where  $w = \frac{1 - \lambda}{\lambda}$ .

The proposed objective indicates that personalization should expand from the pretrained anchor rather than deviate from it, encouraging subject adaptation while preserving the semantic prior. Existing approaches [10, 24, 30] leverage frequent concepts but do not model their interactive relationship with personalized representations. As validated in Section 4, the proposed formulation leads to consistent performance improvements in practice. Furthermore, despite not explicitly targeting prior preservation, our method achieves lower drift from the pretrained representations than prior-preserving baselines, as shown in Figure 2.

## 4. Experiments

In this section, we present experiments and analyses to validate the effectiveness of our method across various subjects and diffusion backbones.

### 4.1. Experimental Setup.

**Implementation Details.** We conduct experiments on the widely used personalization benchmark [30]. The benchmark contains 30 subjects encompassing both objects and live subjects. Each subject provides 4-6 reference images and every model is prompted with 25 distinct textual templates, generating four samples per prompt to evaluate both subject and text consistency. We compare our method against a comprehensive set of state-of-the-art personalization approaches, including DreamBooth [30] (both full fine-tuning and LoRA-based variants), SuDe [24], SVDiff [6], Textual Inversion [5], and Custom Diffusion [12].

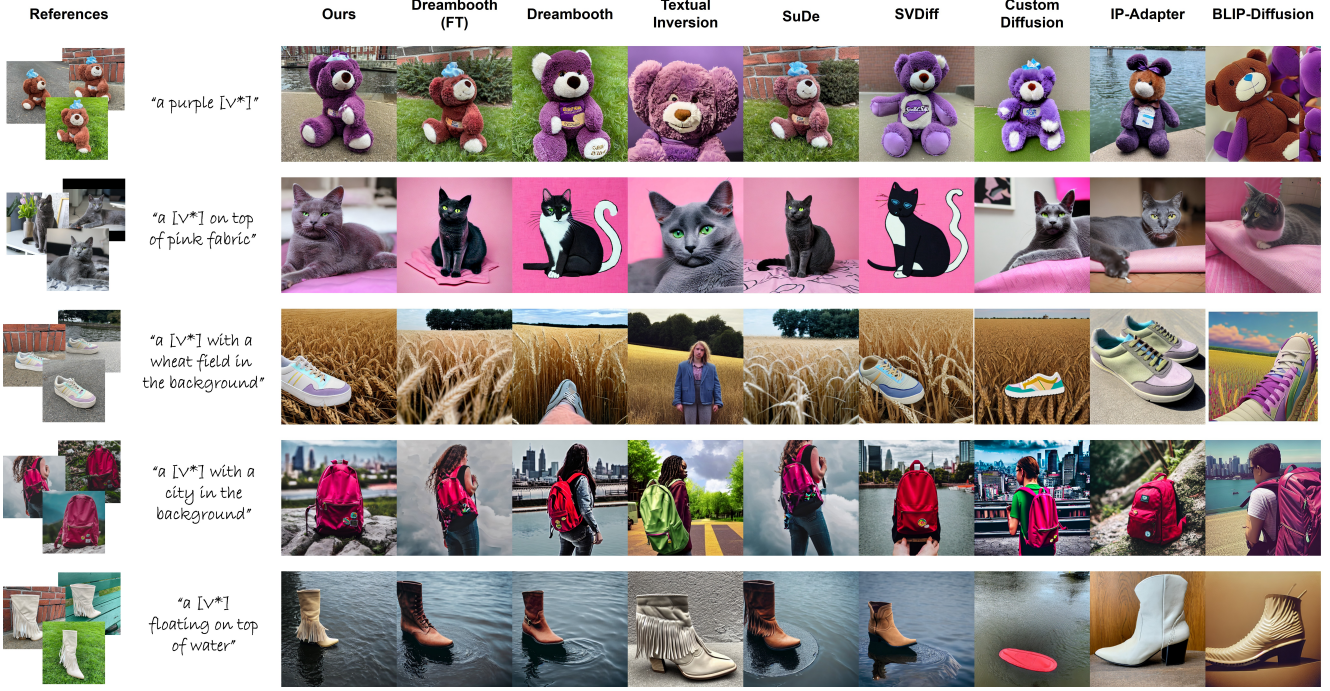


Figure 3. Visual comparison of few-shot personalization and encoder-based methods on the SD1.5 backbone.

To broaden the comparison, we also include encoder-based methods such as IP-Adapter [40] and BLIP-Diffusion [14]. To examine scalability across different model capacities, we conduct experiments on three representative backbones—Stable Diffusion 1.5 (SD1.5) [29], Stable Diffusion XL (SDXL) [22], and Stable Diffusion 3 (SD3) [4]. All fine-tuning experiments adopt LoRA-based adaptation [9] for efficient personalization.

**Evaluation Metrics.** We evaluate the generated results along two dimensions. Subject fidelity, quantified by CLIP-I [26] and DINO [1], measures cosine similarity between image embeddings of generated images and reference samples. Text fidelity measured by CLIP-T, evaluates the text-image alignment through the cosine similarity between the CLIP text and image embeddings.

## 4.2. Comparison with Baseline Methods

Table 1 summarizes quantitative comparisons with baseline personalization methods across subject fidelity and text alignment metrics. Since these two metrics exhibit an inherent trade-off, we also compute a rank-based evaluation by averaging the per-metric ranks of CLIP-I, CLIP-T, and DINO. Our method obtains the top rank under this evaluation, reflecting higher overall performance relative to all baselines. In particular, we observe clear gains over DreamBooth (FT) and SuDe across all metrics. Compared with DreamBooth, our approach notably improves image fi-

Table 1. Quantitative comparison of few-shot personalization and encoder-based methods on the SD1.5 backbone. The Rank column is computed by averaging the per-metric ranks of CLIP-I, CLIP-T, and DINO scores.

Method	CLIP-I ↑	CLIP-T ↑	DINO ↑	Rank
<i>Few-shot personalization methods</i>				
<b>Ours</b>	0.7821	0.3059	0.6031	<b>1</b>
DreamBooth (FT)	0.7751	0.3035	0.5870	4
DreamBooth	0.7302	0.3191	0.4839	6
SuDe	0.7791	0.3044	0.5931	3
SVDiff	0.7455	0.3162	0.5144	5
Textual Inversion	0.7579	0.2633	0.5287	8
Custom Diffusion	0.6479	0.3154	0.5568	7
<i>Encoder-based methods</i>				
IP-Adapter	0.8311	0.2646	0.6290	2
BLIP-Diffusion	0.7016	0.2949	0.4544	9

delity, yielding a more balanced trade-off between subject identity and prompt adherence. This trend is consistent with the qualitative results in Figure 3, where DreamBooth (FT) and SuDe preserve subject identity but fail to follow the prompt, while DreamBooth suffers from incomplete identity preservation.

Further analyses of the quantitative and qualitative results highlight the importance of jointly achieving subject fidelity and prompt alignment. SVDiff and Custom Diffu-

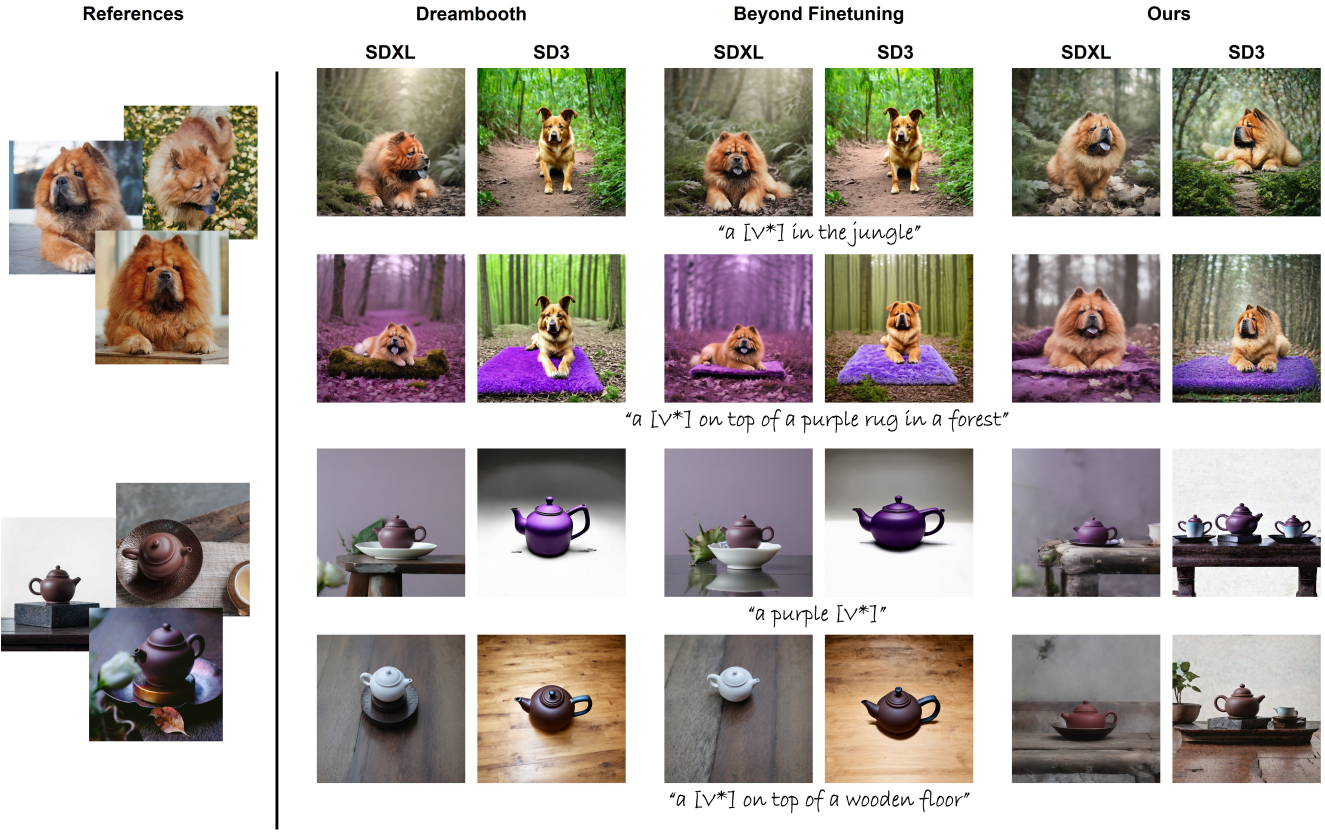


Figure 4. Qualitative comparison on SDXL and SD3 backbones among DreamBooth, Beyond-Finetuning, and our method.

sion exhibit strong prompt adherence and obtain high text-related scores, but their subject identity is often unstable. In contrast, Text Inversion and IP-Adapter maintain reasonable identity scores, yet closer examination shows that they preserve only coarse characteristics, missing fine-grained details, and their prompt following remains inconsistent. Although a slight subject-prompt mixing appears in the second row of Figure 3, the overall visual results preserve subject identity and adhere to the prompt. These observations suggest that the proposed anchoring strategy supports more reliable personalization performance.

### 4.3. Comparison across Backbone Models

To assess the generalization of our method across architectures, we compare it against DreamBooth and the inference-only anchoring approach, Beyond-Finetuning [35], across SD1.5, SDXL, and SD3 backbones, as shown in Table 2. For Beyond-Finetuning, we follow its switching sampling strategy with the same hyperparameter setup. We also compute an overall rank using the same procedure as in Table 1.

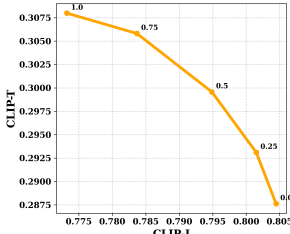
Across all backbones, our approach outperforms both baselines and consistently attains the top rank. On SDXL, our method achieves the highest scores in all metrics. On SD1.5 and SD3, it preserves strong text alignment

Table 2. Quantitative comparison on SD1.5, SDXL, and SD3 backbones, augmented with an overall rank column.

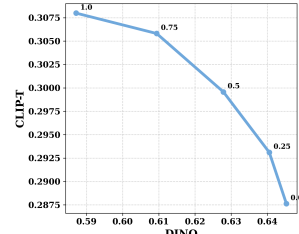
Model	Method	CLIP-I $\uparrow$	CLIP-T $\uparrow$	DINO $\uparrow$	Rank
SD1.5	DreamBooth	0.7302	0.3191	0.4839	2
	Beyond-Finetuning	0.7293	<b>0.3212</b>	0.4786	3
	<b>Ours</b>	<b>0.7821</b>	0.3059	<b>0.6031</b>	<b>1</b>
SDXL	DreamBooth	0.7939	0.3107	0.6586	2
	Beyond-Finetuning	0.7874	0.3140	0.6429	3
	<b>Ours</b>	<b>0.8005</b>	<b>0.3154</b>	<b>0.6661</b>	<b>1</b>
SD3	DreamBooth	0.7465	0.3182	0.5130	2
	Beyond-Finetuning	0.7461	<b>0.3211</b>	0.4997	3
	<b>Ours</b>	<b>0.7579</b>	0.3187	<b>0.5679</b>	<b>1</b>

while yielding larger gains in image fidelity compared with DreamBooth and Beyond-Finetuning. The findings support our central claim that anchoring must be incorporated during training rather than applied only at inference. Learning personalized guidance in the presence of an anchor allows the model to maintain the connection between general and subject specific representations, which leads to improved performance across various architectures.

Qualitative results further support these findings as illustrated in Figure 4. In the first examples, both Dream-



(a) Relationship between CLIP-I and CLIP-T under varying  $w$



(b) Relationship between DINO and CLIP-T under varying  $w$

Figure 5. Analysis of subject fidelity and text alignment under different weighting parameters  $w$ .

Booth and Beyond-Finetuning under the SD3 backbone fail to preserve subject identity, yielding distorted facial features. Although Beyond-Finetuning improves CLIP-T, its identity still deviate from the reference because its strategy affects only the sampling process. These results highlight DreamBooth’s poor generalization and the limited impact of Beyond-Finetuning’s post-hoc correction. In contrast, our method reproduces distinctive details such as fur color, snout shape, and posture, while maintaining contextual cues (“a [V\*] on top of a purple rug in a forest”), leading to the highest CLIP-I and DINO scores. A similar pattern is observed in the teapot examples (third and fourth rows). These results demonstrate that our semantic-anchored training aligns subject and anchor representations through optimization, yielding robust and perceptually faithful adaptation across diffusion backbones.

## 5. Ablation Studies

In this section, we perform ablation studies to analyze the contribution of each component in semantic anchoring and its impact on the overall personalization process. We first examine how varying the anchoring strength influences performance, providing insight into the role of the anchoring term. We then analyze the personalization trajectory to understand how the proposed objective shapes the Semantic Space Dynamics and its resulting implications. Furthermore, we examine the effect of applying an inference-time anchoring strategy to our method, allowing us to observe the role of train-test anchoring alignment.

### 5.1. Anchoring Effect on Personalization

We investigate how varying the anchoring weight affects the balance between subject fidelity and semantic alignment. In Eq. (5),  $w$  controls the relative contribution between the reconstruction loss and the semantic anchoring loss. We vary the weight ( $w \in \{0.0, 0.25, 0.5, 0.75, 1.0\}$ ) to investigate its influence. As illustrated in Figure 5, increasing  $w$  enhances CLIP-T while reducing CLIP-I and DINO, reveal-

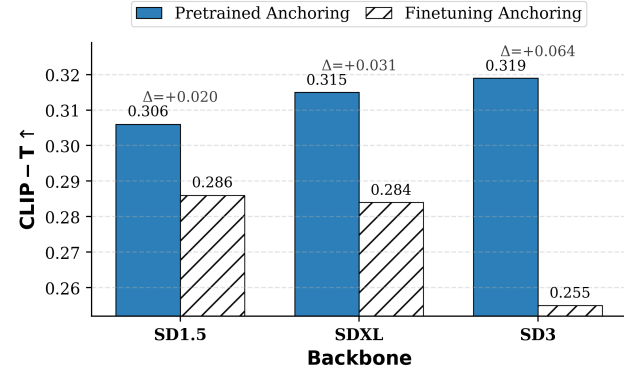


Figure 6. Comparison of semantic alignment (CLIP-T) using two different anchoring strategies. Pretrained anchoring attains higher CLIP-T scores than finetuned anchoring.

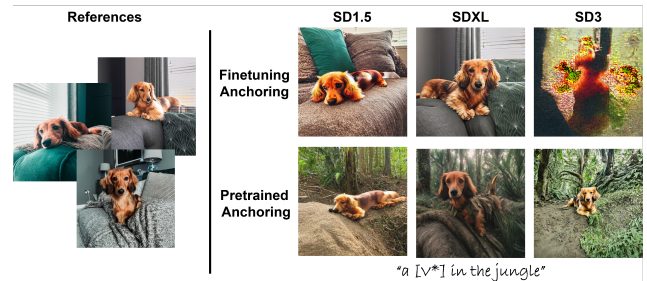


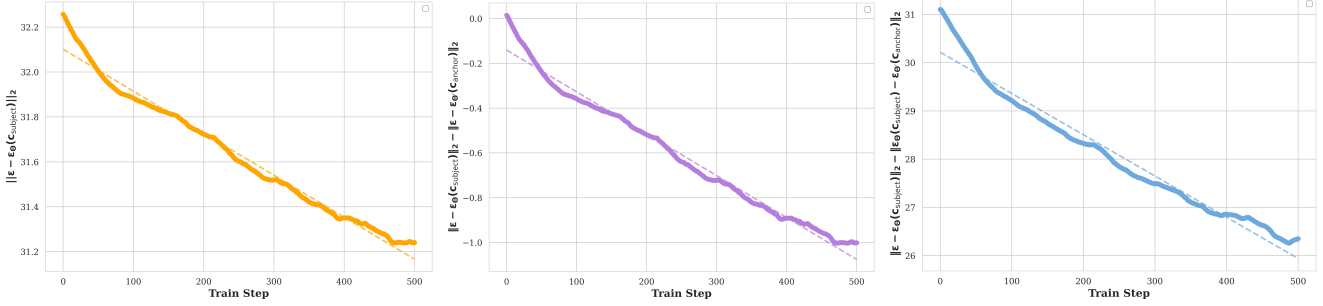
Figure 7. Comparison of qualitative results using two different anchoring strategies. Both preserve subject fidelity, and the pretrained anchoring shows better consistency to the text description.

ing a smooth balance trajectory between semantic alignment and subject fidelity. This indicates that  $w$  determines the interpolation strength between the subject-specific distribution and the pretrained anchor representation. The optimal region appears around  $w = 0.5$ , where the interpolation between subject and pretrained anchor achieves the best compromise, maintaining both visual fidelity and semantic consistency. This tendency supports our formulation, showing that balancing subject-specific semantics with the pretrained prior stabilizes the personalization process.

### 5.2. Anchoring Strategy

In this section, we investigate the appropriate anchoring strategy for our method. In Eq. (5), the anchor term  $\epsilon_{\theta'}(z_t, c^{\text{anc}}, t)$  is obtained from the pretrained model  $\theta'$  throughout personalization. To examine the role of anchoring, we conduct an additional experiment in which the anchor is instead taken from the current personalized model  $\theta$ . This setup isolates the effect of anchoring the subject model to the pretrained distribution and enables a focused analysis of its role in text-image alignment.

As a result, the pretrained anchor configuration consistently achieves higher CLIP-T scores across all backbones



(a) Distance between reference and subject prediction. (b) Difference of distances between reference and subject and reference-anchor. (c) Difference of distances between subject reference and subject-anchor.

Figure 8. Analysis of distance relationships among reference, subject, and anchor predictions. The semantic dynamics observed during personalization indicate that the proposed method evolves from the pretrained anchor.

in Figure 6. Since text coherence reflects the pretrained semantic knowledge, these results indicate that preserving the pretrained reference is essential for maintaining the original contextual semantics. When the anchor reference is also finetuned, both the subject and anchor predictions evolve simultaneously, causing the semantic reference point to drift. Consequently, the model loses text alignment capability. This observation aligns with the principle formalized in Eq. (3), where the frequent concept should remain stable while the rare concept is newly learned. These findings demonstrate that the proposed anchoring strategy effectively preserves this relationship over personalization.

### 5.3. Semantic Space Dynamics

To better understand the semantic space dynamics, we analyze the pairwise distances between the components of our objective function. This analysis reveals how the proposed objective evolves during training and explains the source of its performance improvement. As shown in Figure 8a, we first examine how well the personalized guidance  $\epsilon_\theta(z_t, c^{sbj}, t)$  is learned by measuring  $\|\epsilon - \epsilon_\theta(z_t, c^{sbj}, t)\|_2$ . The distance decreases as training progresses, indicating that the subject-specific attributes are gradually encoded into the personalized representation. Next, Figure 8b reveals the position of the personalized guidance within the semantic space. The personalized representation starts near the pretrained anchor prediction  $\epsilon_\theta(z_t, c^{cls}, t)$  and shifts as it learns subject-specific semantics. This behavior reflects the R2F-based guidance assumption, where personalization corresponds to the rare concept that expands from the frequent anchor.

Figure 8c and Figure 2 shows that the proposed objective enables efficient training and performance improvement. As shown in Figure 8c the proposed objective exhibits stable convergence during personalization with the loss decreasing as training progresses. At the same time, Figure 2 shows that our method achieves strong personal-

ization while maintaining minimal shift from the pretrained prior. This confirms that our approach expands from the anchor concept with minimal drift, enabling efficient learning and stable semantic alignment as shown in Section 4.

## 6. Conclusion

In this paper, we reformulate personalization as a problem of learning a rare concept guided by a frequent one. Rather than optimizing subject-specific reconstruction and pretrained knowledge preservation independently, we introduce a relational objective that explicitly anchors the novel concept to its semantic superclass. This anchoring perspective enables personalization to expand from the pretrained semantic structure while retaining its contextual coherence. Our method demonstrates strong improvements in both text alignment and image fidelity across a wide range of baselines, and we further validate its generality on various backbone models. Through comprehensive ablation studies, we analyze the internal dynamics of our objective and show that it behaves as predicted by the formulation. In conclusion, we present Semantic Anchoring Personalization, a novel method that leverages the relationship between general and subject-specific concepts, offering a more reliable and semantically consistent personalization scheme.

**Discussion and Future Work.** Our findings demonstrate that introducing a semantic anchor offers a principled way to structure the interaction between pretrained and subject-specific representations. While our formulation anchors each subject to its superclass semantics, the appropriate granularity and adaptiveness of this anchoring remain open questions. Exploring richer semantic structures and understanding how different semantic factors contribute to each subject’s adaptation dynamics presents a promising direction for future work.

## References

[1] Mathilde Caron, Hugo Touvron, Ishan Misra, Hervé Jégou, Julien Mairal, Piotr Bojanowski, and Armand Joulin. Emerging properties in self-supervised vision transformers. In *Proceedings of the IEEE/CVF international conference on computer vision*, pages 9650–9660, 2021. 5

[2] Prafulla Dhariwal and Alexander Nichol. Diffusion models beat gans on image synthesis. *Advances in neural information processing systems*, 34:8780–8794, 2021. 2

[3] Bradley Efron. Tweedie’s formula and selection bias. *Journal of the American Statistical Association*, 106(496):1602–1614, 2011. “Tweedie’s formula, first reported by Robbins in 1956, offers a simple empirical Bayes approach for correcting selection bias.”. 4

[4] Patrick Esser, Sumith Kulal, Andreas Blattmann, Rahim Entezari, Jonas Müller, Harry Saini, Yam Levi, Dominik Lorenz, Axel Sauer, Frederic Boesel, et al. Scaling rectified flow transformers for high-resolution image synthesis. In *Forty-first international conference on machine learning*, 2024. 1, 5

[5] Rinon Gal, Yuval Alaluf, Yuval Atzmon, Or Patashnik, Amit H Bermano, Gal Chechik, and Daniel Cohen-Or. An image is worth one word: Personalizing text-to-image generation using textual inversion. *arXiv preprint arXiv:2208.01618*, 2022. 1, 2, 4

[6] Ligong Han, Yinxiao Li, Han Zhang, Peyman Milanfar, Dimitris Metaxas, and Feng Yang. Svdiff: Compact parameter space for diffusion fine-tuning. In *Proceedings of the IEEE/CVF International Conference on Computer Vision*, pages 7323–7334, 2023. 1, 2, 4

[7] Jonathan Ho and Tim Salimans. Classifier-free diffusion guidance. *arXiv preprint arXiv:2207.12598*, 2022. 2

[8] Jonathan Ho, Ajay Jain, and Pieter Abbeel. Denoising diffusion probabilistic models. *Advances in neural information processing systems*, 33:6840–6851, 2020. 3

[9] Edward J Hu, Yelong Shen, Phillip Wallis, Zeyuan Allen-Zhu, Yuanzhi Li, Shean Wang, Lu Wang, Weizhu Chen, et al. Lora: Low-rank adaptation of large language models. *ICLR*, 1(2):3, 2022. 1, 2, 5

[10] Jiannan Huang, Jun Hao Liew, Hanshu Yan, Yuyang Yin, Yao Zhao, Humphrey Shi, and Yunchao Wei. Classdiffusion: More aligned personalization tuning with explicit class guidance. *arXiv preprint arXiv:2405.17532*, 2024. 3, 4

[11] Tero Karras, Miika Aittala, Tuomas Kynkänniemi, Jaakko Lehtinen, Timo Aila, and Samuli Laine. Guiding a diffusion model with a bad version of itself. *Advances in Neural Information Processing Systems*, 37:52996–53021, 2024. 2

[12] Nupur Kumari, Bingliang Zhang, Richard Zhang, Eli Shechtman, and Jun-Yan Zhu. Multi-concept customization of text-to-image diffusion. In *Proceedings of the IEEE/CVF conference on computer vision and pattern recognition*, pages 1931–1941, 2023. 1, 2, 4

[13] Tuomas Kynkänniemi, Miika Aittala, Tero Karras, Samuli Laine, Timo Aila, and Jaakko Lehtinen. Applying guidance in a limited interval improves sample and distribution quality in diffusion models. *Advances in Neural Information Processing Systems*, 37:122458–122483, 2024. 2

[14] Dongxu Li, Junnan Li, and Steven Hoi. Blip-diffusion: Pre-trained subject representation for controllable text-to-image generation and editing. *Advances in Neural Information Processing Systems*, 36:30146–30166, 2023. 2, 5

[15] Junnan Li, Dongxu Li, Caiming Xiong, and Steven Hoi. Blip: Bootstrapping language-image pre-training for unified vision-language understanding and generation. In *International conference on machine learning*, pages 12888–12900. PMLR, 2022. 2

[16] Junnan Li, Dongxu Li, Silvio Savarese, and Steven Hoi. Blip-2: Bootstrapping language-image pre-training with frozen image encoders and large language models. In *International conference on machine learning*, pages 19730–19742. PMLR, 2023. 2

[17] Calvin Luo. Understanding diffusion models: A unified perspective. *arXiv preprint arXiv:2208.11970*, 2022. 3

[18] Alexander Quinn Nichol and Prafulla Dhariwal. Improved denoising diffusion probabilistic models. In *International conference on machine learning*, pages 8162–8171. PMLR, 2021. 3

[19] Dongmin Park, Sebin Kim, Taehong Moon, Minkyu Kim, Kangwook Lee, and Jaewoong Cho. Rare-to-frequent: Unlocking compositional generation power of diffusion models on rare concepts with llm guidance. *arXiv preprint arXiv:2410.22376*, 2024. 2, 3

[20] Sunghyun Park, Seokeon Choi, Hyoungwoo Park, and Sungrack Yun. Steering guidance for personalized text-to-image diffusion models. In *Proceedings of the IEEE/CVF International Conference on Computer Vision*, pages 15907–15916, 2025. 2

[21] Prin Phunyaphibarn, Phillip Y Lee, Jaihoon Kim, and Minhyuk Sung. Unconditional priors matter! improving conditional generation of fine-tuned diffusion models. *arXiv preprint arXiv:2503.20240*, 2025. 2

[22] Dustin Podell, Zion English, Kyle Lacey, Andreas Blattmann, Tim Dockhorn, Jonas Müller, Joe Penna, and Robin Rombach. Sdxl: Improving latent diffusion models for high-resolution image synthesis. *arXiv preprint arXiv:2307.01952*, 2023. 1, 5

[23] Senthil Purushwalkam, Akash Gokul, Shafiq Joty, and Nikhil Naik. Bootpig: Bootstrapping zero-shot personalized image generation capabilities in pretrained diffusion models. In *European Conference on Computer Vision*, pages 252–269. Springer, 2024. 2

[24] Pengchong Qiao, Lei Shang, Chang Liu, Baigui Sun, Xiangyang Ji, and Jie Chen. Facechain-sude: Building derived class to inherit category attributes for one-shot subject-driven generation. In *Proceedings of the IEEE/CVF Conference on Computer Vision and Pattern Recognition*, pages 7215–7224, 2024. 3, 4

[25] Zeju Qiu, Weiyang Liu, Haiwen Feng, Yuxuan Xue, Yao Feng, Zhen Liu, Dan Zhang, Adrian Weller, and Bernhard Schölkopf. Controlling text-to-image diffusion by orthogonal finetuning. *Advances in Neural Information Processing Systems*, 36:79320–79362, 2023. 1, 2

[26] Alec Radford, Jong Wook Kim, Chris Hallacy, Aditya Ramesh, Gabriel Goh, Sandhini Agarwal, Girish Sastry,

Amanda Askell, Pamela Mishkin, Jack Clark, et al. Learning transferable visual models from natural language supervision. In *International conference on machine learning*, pages 8748–8763. PMLR, 2021. 5

[27] Aditya Ramesh, Mikhail Pavlov, Gabriel Goh, Scott Gray, Chelsea Voss, Alec Radford, Mark Chen, and Ilya Sutskever. Zero-shot text-to-image generation. In *International conference on machine learning*, pages 8821–8831. Pmlr, 2021. 1

[28] Aditya Ramesh, Prafulla Dhariwal, Alex Nichol, Casey Chu, and Mark Chen. Hierarchical text-conditional image generation with clip latents. *arXiv preprint arXiv:2204.06125*, 1(2):3, 2022.

[29] Robin Rombach, Andreas Blattmann, Dominik Lorenz, Patrick Esser, and Björn Ommer. High-resolution image synthesis with latent diffusion models. In *Proceedings of the IEEE/CVF conference on computer vision and pattern recognition*, pages 10684–10695, 2022. 1, 5

[30] Nataniel Ruiz, Yuanzhen Li, Varun Jampani, Yael Pritch, Michael Rubinstein, and Kfir Aberman. Dreambooth: Fine tuning text-to-image diffusion models for subject-driven generation. In *Proceedings of the IEEE/CVF conference on computer vision and pattern recognition*, pages 22500–22510, 2023. 1, 2, 3, 4

[31] Dvir Samuel, Rami Ben-Ari, Nir Darshan, Haggai Maron, and Gal Chechik. Norm-guided latent space exploration for text-to-image generation. *Advances in Neural Information Processing Systems*, 36:57863–57875, 2023. 2

[32] Dvir Samuel, Rami Ben-Ari, Simon Raviv, Nir Darshan, and Gal Chechik. Generating images of rare concepts using pre-trained diffusion models. In *Proceedings of the AAAI Conference on Artificial Intelligence*, pages 4695–4703, 2024. 2

[33] Christoph Schuhmann, Romain Beaumont, Richard Vencu, Cade Gordon, Ross Wightman, Mehdi Cherti, Theo Coombes, Aarush Katta, Clayton Mullis, Mitchell Wortsman, et al. Laion-5b: An open large-scale dataset for training next generation image-text models. *Advances in neural information processing systems*, 35:25278–25294, 2022. 1

[34] Jing Shi, Wei Xiong, Zhe Lin, and Hyun Joon Jung. Instantbooth: Personalized text-to-image generation without test-time finetuning. In *Proceedings of the IEEE/CVF conference on computer vision and pattern recognition*, pages 8543–8552, 2024. 2

[35] Vera Soboleva, Maksim Nakhodnov, and Aibek Alanov. Beyond fine-tuning: A systematic study of sampling techniques in personalized image generation. *arXiv preprint arXiv:2502.05895*, 2025. 2, 3, 6

[36] Jiaming Song, Chenlin Meng, and Stefano Ermon. Denoising diffusion implicit models. *arXiv preprint arXiv:2010.02502*, 2020. 3

[37] Yang Song, Jascha Sohl-Dickstein, Diederik P Kingma, Abhishek Kumar, Stefano Ermon, and Ben Poole. Score-based generative modeling through stochastic differential equations. *arXiv preprint arXiv:2011.13456*, 2020. 3, 4

[38] Yoad Tewel, Rinon Gal, Gal Chechik, and Yuval Atzmon. Key-locked rank one editing for text-to-image personalization. In *ACM SIGGRAPH 2023 conference proceedings*, pages 1–11, 2023. 1, 3

[39] Soobin Um and Jong Chul Ye. Minority-focused text-to-image generation via prompt optimization. In *Proceedings of the Computer Vision and Pattern Recognition Conference*, pages 20926–20936, 2025. 2

[40] Hu Ye, Jun Zhang, Sibo Liu, Xiao Han, and Wei Yang. Ipt-adapter: Text compatible image prompt adapter for text-to-image diffusion models. *arXiv preprint arXiv:2308.06721*, 2023. 2, 5

[41] Yu Zeng, Vishal M Patel, Haochen Wang, Xun Huang, Ting-Chun Wang, Ming-Yu Liu, and Yogesh Balaji. Jedi: Joint-image diffusion models for finetuning-free personalized text-to-image generation. In *Proceedings of the IEEE/CVF Conference on Computer Vision and Pattern Recognition*, pages 6786–6795, 2024. 2